

PAPER • OPEN ACCESS

## Enhanced mechanical properties in fully recrystallized ultrafine grained ZKX600 Mg alloy

To cite this article: Ruixiao Zheng *et al* 2017 *IOP Conf. Ser.: Mater. Sci. Eng.* **219** 012055

View the [article online](#) for updates and enhancements.

### Related content

- [Change of deformation mechanisms in ultrafine grained Mg-Zn-Zr-Ca alloy](#)  
Ruixiao Zheng, Tilak Bhattacharjee, Akinobu Shibata *et al.*
- [Effect of severe plastic deformation on the structure and properties of Ni-Cu alloys](#)  
V V Popov, A V Stolbolsky and E N Popova
- [A Versatile Method for Nanostructuring Metals, Alloys and Metal Based Composites](#)  
G Gurau, C Gurau, L G Bujoreanu *et al.*



**IOP | ebooks™**

Bringing you innovative digital publishing with leading voices to create your essential collection of books in STEM research.

Start exploring the collection - download the first chapter of every title for free.

# Enhanced mechanical properties in fully recrystallized ultrafine grained ZKX600 Mg alloy

Ruixiao Zheng<sup>1</sup>, Tilak Bhattacharjee<sup>1,2</sup>, Si Gao<sup>1</sup>, Wu Gong<sup>2</sup>, Akinobu Shibata<sup>1,2</sup>, Taisuke Sasaki<sup>3</sup>, Kazuhiro Hono<sup>3</sup> and Nobuhiro Tsuji<sup>1,2</sup>

<sup>1</sup> Department of Materials Science and Engineering, Kyoto University, Yoshida Honmachi, Sakyo-ku, Kyoto 606-8501, Japan

<sup>2</sup> Elements Strategy Initiative for Structural Materials (ESISM), Kyoto University

<sup>3</sup> National Institute for Materials Science, 1-2-1 Sengen, Tsukuba 305-0047, Japan

E-mail: zheng.ruixiao.7m@kyoto-u.ac.jp

**Abstract.** Mg-Zn-Zr-Ca (ZKX600) alloy specimens with various fully recrystallized grain sizes ranging from 0.77  $\mu\text{m}$  to 23.3  $\mu\text{m}$  were fabricated by high pressure torsion (HPT) followed by subsequent annealing. Tensile tests carried out at room temperature revealed that ultrafine grained (UFG) specimens exhibited enhanced combinations of strength and ductility compared to their coarse-grained counterparts. Observation of deformation microstructures suggested that basal slip and  $\{10\text{-}12\}$  extension twinning were the dominant mechanisms during deformation of coarse grained specimens, while deformation twinning was significantly inhibited in the UFG specimens. Based on the observations it is proposed that non-basal slip activity is responsible for the enhanced mechanical properties, and should be the focus of further investigations.

## 1. Introduction

Due to their ultra-low density, and high specific strength, magnesium (Mg) alloys have been increasingly used as structural components in the automotive and aerospace industries to achieve weight reduction and fuel economy improvements [1-3]. However, their anisotropic hexagonal close packed (HCP) crystallographic structure provides only a limited number of independent deformation modes, resulting in relatively low tensile ductility as well as poor formability at room temperature [4].

Grain refinement is considered as one of the promising ways for optimizing the strength of Mg alloys without sacrificing ductility [5]. However, the microstructures of Mg alloys refined by conventional processes (such as rolling and extrusion) are usually inhomogeneous and the mean grain sizes are usually above 10  $\mu\text{m}$ . In contrast, severe plastic deformation (SPD) processes, such as equal channel angular pressing (ECAP), accumulative roll bonding (ARB) and high pressure torsion (HPT), have already been proven as effective approaches for realizing ultra-grain refinement in various metallic materials [6]. It is, however, quite challenging to refine the grain size of Mg alloys by using ECAP and ARB because of cracking and fracture during heavy deformation. For example, Cetlin *et al.* [7] have shown very clear examples of serious segmentation in an annealed ZK60 Mg alloy and an extruded AZ31 Mg alloy processed by ECAP only after one pass at different temperatures.

In contrast, a high hydrostatic pressure is applied to disc-shaped specimens during torsion deformation in HPT, so that undesirable cracking can be avoided even at room temperature [8].



Recently, Meng *et al.* [9] carried out HPT deformation of a Mg-3.4Zn (at.%) alloy at ambient temperature and found that equiaxed grains with an average diameter of 140 nm could be obtained after HPT by 20 revolutions. However, due to the high density of retained lattice defects such as dislocations, the HPT-processed UFG Mg alloys did not show good ductility. Thus, their mechanical properties were characterized only by using simple hardness testing. Such a limited ductility resulting from the characteristics of the deformed microstructure is a common feature of SPD-processed metallic materials.

In order to overcome the above deficiency of HPT-processed Mg alloys, a process including room temperature HPT followed by a subsequent annealing treatment is proposed in the present study. A Mg-Zn-Zr-Ca (ZKX600) alloy is selected for realizing optimal nanostructures, because this alloy contains a high density of thermally stable nano-precipitates even in the as-cast state. It is expected that these nano-precipitates should be effective for controlling the grain size during thermo-mechanical processes.

## 2. Experimental Procedures

An as-received ZKX600 Mg alloy ingot with a composition of Mg-6.2%Zn-0.5%Zr-0.2%Ca (mass%) was firstly homogenized at 350 °C for 48 h followed by a solid solution treatment at 400 °C for 1 h using a box-type resistance furnace. Disc-shaped samples with a diameter of 10 mm and thickness of 0.80 mm were cut from the ingot for HPT. The HPT deformation was conducted at room temperature under a compressive pressure of 6 GPa at a rotation speed of 0.2 rpm. The total rotation angle applied was 360°. After the HPT process, the specimens were given an annealing treatment at various temperatures for different periods of time, using a salt bath furnace.

The areas at a radial distance of 3.0 mm from the center on transverse sections containing the rotation axis of the HPT-processed discs were observed by transmission electron microscopy (TEM) using a JEOL 2010 microscope operated at 200 kV. The areas at a distance of 3.0 mm from the center on sections perpendicular to the rotation axis of the annealed discs were characterized by field emission scanning electron microscopy (FE-SEM) using a JSM 7100F scanning electron microscope equipped with an electron backscatter diffraction (EBSD) system. Grain sizes were measured using a linear intercept method based on the obtained EBSD maps.

The mechanical properties of the specimens were characterized by uniaxial tensile testing. Small-sized tensile specimens with a gauge length of 2 mm and a cross section of 1 mm × 0.5 mm were cut from the discs such that the center of the gauge length was coincident with a radial distance of 2.5 mm from the center of the HPT disks with the tensile direction taken perpendicular to the radial direction of the discs. Tensile tests were carried out at a quasi-static strain rate of  $8.3 \times 10^{-4} \text{ s}^{-1}$ , with a direct measurement of the displacement of the gauge section using a CCD video camera extensometer.

## 3. Results and Discussion

Figure 1 shows microstructures of the as-solution treated (ST) (a,b), 180° HPT-processed (c), and 360° HPT-processed (d) specimens. Figure 1(a) is an EBSD inverse pole figure (IPF) map indicating crystallographic orientations parallel to the normal direction of the as-ST disc specimen. The EBSD-IPF map reveals that the as-ST specimen has a coarse grained structure with a mean grain size of about 57 μm and did not have strong crystallographic texture. TEM observation (figure 1(b)) indicated that a high density of rod-shaped nano-precipitates ( $\beta$ -phase) with an average length of 35 nm are retained, even after the solution treatment [10]. After HPT by 180°, an ultrafine lamellar structure, elongated along the shear direction, was obtained. The mean spacing of the lamellar boundaries was about 100 nm, as indicated by the dark field TEM image shown in figure 1(c). After further deformation by HPT to 360°, the lamellar structure was fragmented and replaced by a nearly equiaxed nanocrystalline structure, as shown in figure 1(d). The mean grain size of the nanocrystals was about 100 nm, which is significantly finer than that of pure Mg (grain size ~1 μm) subjected to the HPT process up to similar rotation angles [11]. The result indicates that the alloying elements in the present Mg alloy play an important role in reducing the grain size that can be obtained by SPD.

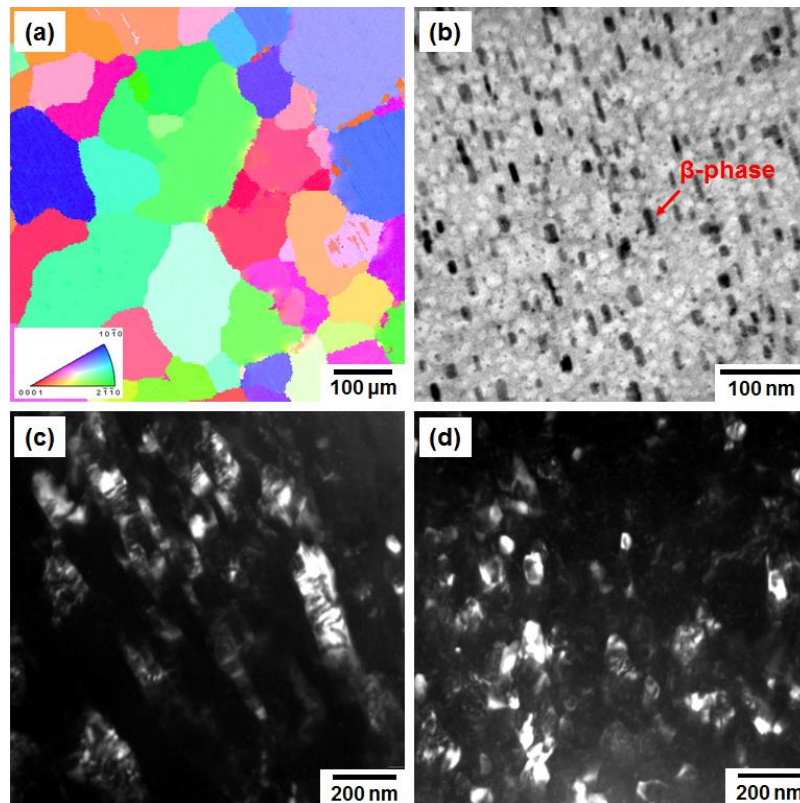


**Figure 1.** (a) EBSD-IPF map and (b) bright field TEM image of the as-ST specimen showing a coarse grained structure with a mean grain size of 57  $\mu\text{m}$  and a high density of nano-precipitates ( $\beta$ -phase). (c) Dark field TEM image of the 180° HPT processed specimen showing an ultrafine lamellar structure. (d) Dark field TEM image of the 360° HPT processed specimen showing a nearly equiaxed nanocrystalline structure with a mean grain size of about 100 nm.

Figure 2 shows EBSD results of the specimen HPT-processed by 360° and then annealed at 400 °C for 1 min (a-c) and 500 °C for 30 min (d-f). The colors in the IPF maps (a, d) indicate crystallographic orientations parallel to the normal direction of the HPT discs. The blue and green lines in the grain boundary (GB) maps (b, e) correspond to high angle grain boundaries (HAGBs) having misorientations larger than 15° and low angle grain boundaries (LAGBs) with misorientations between 2° and 15°. After rapid annealing at 400 °C for 1 min, a fully recrystallized UFG structure with a mean grain size of 0.98  $\mu\text{m}$  was successfully obtained (figure 2(a,b)). In addition, the peak intensity in the (0001) pole figure (figure 2(c)) is low and the peak intensity regions located far from the center of the pole figure, indicating that the strong basal texture usually observed in wrought Mg alloys was not seen in the present annealed specimen. After the high temperature annealing at 500 °C for 30 min, a coarse grained specimen with a mean grain size of 23.3  $\mu\text{m}$  was obtained (figure 2(d,e)) and the texture was further weakened and randomized (figure 2(f)).

For understanding the mechanical properties of the alloy processed under different conditions, tensile testing was carried out on specimens with various grain sizes. The resulting nominal stress-strain curves are presented in figure 3. The 360° HPT-processed specimen ( $d = 0.1 \mu\text{m}$ ) showed a very high yield strength (YS, 0.2% offset of nominal stress) of 311 MPa, but the stress-strain curve became unstable immediately after yielding, resulting in a quite limited tensile elongation of 1.2%. This is typical of the mechanical behavior of nanocrystalline or UFG materials having deformed microstructures [12]. It should be noted, on the other hand, that fully recrystallized UFG specimens

showed very good combination of strength and ductility. In particular, the YS, ultimate tensile strength (UTS), uniform elongation and total elongation of the specimen having a mean grain size of  $0.77\ \mu\text{m}$  were 235 MPa, 328 MPa, 20.5% and 26.1%, respectively. The results clearly demonstrate that by making the microstructure a fully recrystallized UFG, the tensile ductility can be remarkably retained without sacrificing the tensile strength. With increasing grain size, the YS decreases, but the ductility (total elongation) remains almost constant for mean grain sizes smaller than  $6.11\ \mu\text{m}$ . Further increasing the grain size results in a simultaneous decrease in strength and ductility. For instance, the YS, UTS, uniform elongation and total elongation of the specimen with mean grain size of  $23.3\ \mu\text{m}$  are 90 MPa, 256 MPa, 17.6% and 20.3%, respectively.

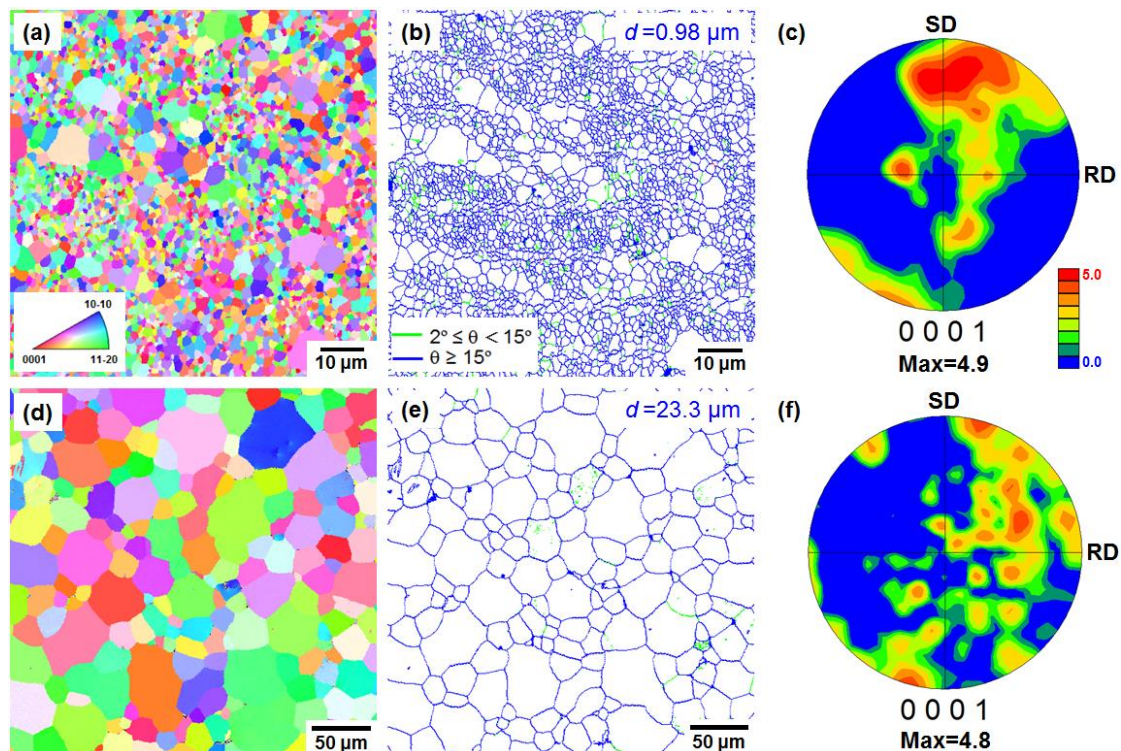


**Figure 2.** (a, d) IPF maps, (b, e) GB maps and (c, f) (0001) pole figures obtained from EBSD measurements and analysis of the specimens HPT-processed by  $360^\circ$  rotation and then annealed at (a-c)  $400\ ^\circ\text{C}$  for 1 min and (d-f)  $500\ ^\circ\text{C}$  for 30 min. SD and RD in the pole figures represent the shear direction and the radial direction, respectively.

In order to reveal the underlying deformation mechanisms contributing to the enhanced tensile ductility in the fully recrystallized UFG specimens, the deformation microstructures were observed after tensile deformation to specified strains. Figure 4 shows EBSD-IPF maps of a coarse grained specimen ( $d = 23.3\ \mu\text{m}$ ) and an UFG specimen ( $d = 0.98\ \mu\text{m}$ ) after tensile deformation to similar strains. Colors in the IPF maps indicate crystallographic orientations parallel to the normal direction of the sheet-type tensile specimens. As shown in figures 4(a) and (b), a high density of deformation twins, with an area fraction of 18.6%, was generated in the coarse grained specimen after a tensile strain of 15%. Crystallographic analysis indicated that the twins were exclusively  $\{10-12\}$  extension twins. It is known that  $\{10-12\}$  extension twinning has much lower critical resolved shear stress than other twinning systems [13]. In contrast, a quite limited number of deformation twins with an area fraction of only 1.5% was seen in the UFG specimen after a similar tensile strain of 14% (see figure 4 (c) and (d)).

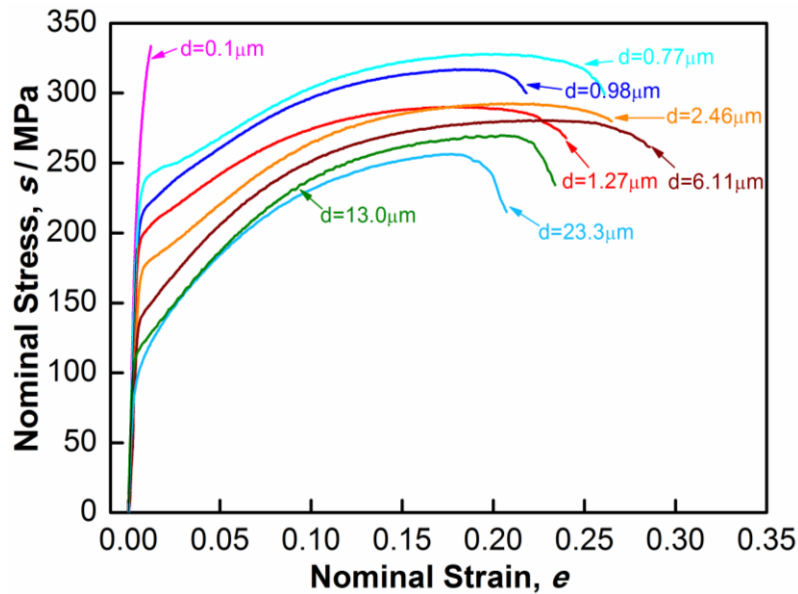


**Figure 3.** Nominal stress-strain curves of specimens with different mean grain sizes.

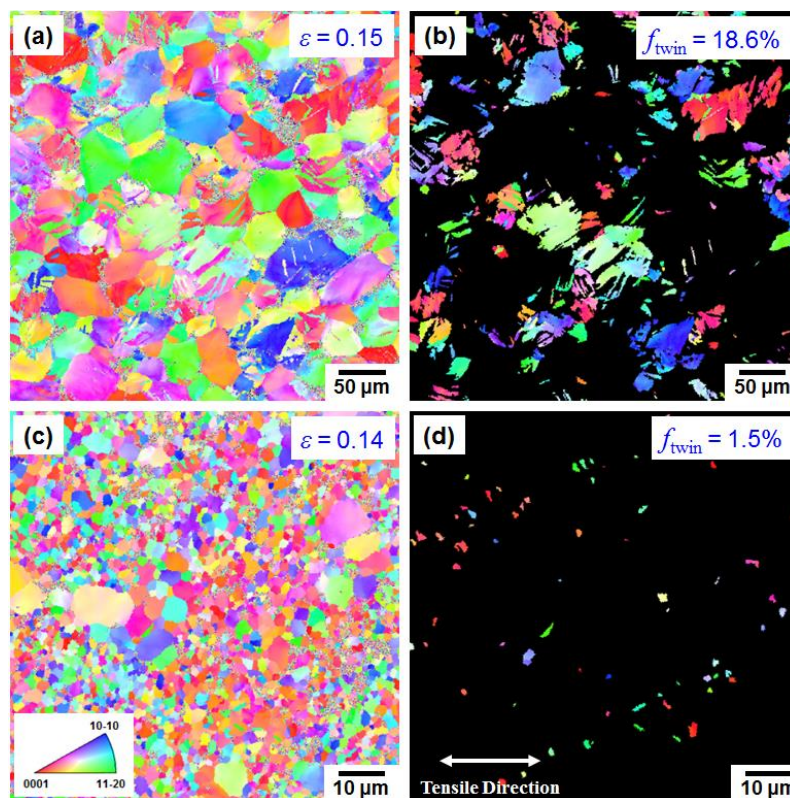


**Figure 4.** EBSD results of (a, b) a coarse grained specimen ( $d = 23.3 \mu\text{m}$ ) and (c, d) an UFG specimen ( $d = 0.98 \mu\text{m}$ ) after tensile deformation to similar strains. (a) IPF map and (b) corresponding twin-partitioned map of the coarse grained specimen after 15% tensile deformation, showing a large area fraction of deformation twins ( $f_{\text{twin}} = 18.6\%$ ). (c) IPF map and (d) corresponding twin-partitioned map of the UFG specimen after 14% tensile deformation, showing a very small area fraction of deformation twins ( $f_{\text{twin}} = 1.5\%$ ).

Although deformation twinning was significantly inhibited in the UFG specimen, the sample exhibited better ductility than the coarse grained specimen. Thus, there must be some other deformation mechanisms responsible for the enhanced strain-hardening and ductility, for example, the activation of non-basal slip systems. Because the Burgers vector of the primary slip system, i.e., basal slip, of Mg and Mg alloys only contains an  $\langle a \rangle$  component, the operation of any deformation mechanism involving a  $\langle c \rangle$  deformation component is necessary for large plasticity. Koike *et al.* [14] reported a large tensile elongation up to 47% in a commercial AZ31 alloy having a mean grain size of 6.5  $\mu\text{m}$ . They concluded that the superior tensile ductility was due to the activation of  $\langle c+a \rangle$  non-basal slip. Similar activation of unusual slip systems that including a  $\langle c \rangle$  component is expected in the present Mg-Zn-Zr-Ca alloy having fully-recrystallized UFG structures. We are planning to make further investigations to clarify this issue in the present material.

#### 4. Conclusion

In summary, fully recrystallized Mg-Zn-Zr-Ca alloy specimens with various mean grain sizes ranging from 0.77  $\mu\text{m}$  to 23.3  $\mu\text{m}$  were successfully fabricated by the combination of HPT and subsequent annealing. Simultaneously enhanced strength and ductility were realized in fully recrystallized UFG specimens. A detailed comparison of the deformation microstructures of an UFG specimen and a coarse-grain specimen clarified that deformation twinning was significantly inhibited in the UFG specimen. It is suggested activation of non-basal slip systems having  $\langle c \rangle$  component plays an important role in the enhanced ductility of recrystallized UFG samples, and this will be investigated further in future studies.

#### Acknowledgments

This work was financially supported by the Elements Strategy Initiative for Structural Materials (ESISM) and the Grant-in-Aid for Scientific Research (S) (No. 15H05767), both through the Ministry of Education, Culture, Sports, Science and Technology (MEXT), Japan.

#### References

- [1] Kim N 2014 *Mater. Sci. Technol.* **30** 1925
- [2] Suh B, Shim M, Shin K and Kim N 2014 *Scr. Mater.* **84** 1
- [3] Hono K, Mendis C, Sasaki T and Oh-Ishi K 2010 *Scr. Mater.* **63** 710
- [4] Agnew S and Nie J 2010 *Scr. Mater.* **63** 671
- [5] Kim W, Jeong H and Jeong H 2009 *Scr. Mater.* **61** 1040
- [6] Tsuji N, Saito Y, Lee Y and Minamino Y 2003 *Adv. Eng. Mater.* **5** 338
- [7] Cetlin P, Aguilar M, Figueiredo R and Longdon T 2010 *J. Mater. Sci.* **45** 4561
- [8] Zhilyaev A and Langdon T 2008 *Prog. Mater. Sci.* **53** 893
- [9] Meng F, Rosalie J, Singh A, Somekawa H and Tsuchiya K 2014 *Scr. Mater.* **78** 57
- [10] Bhattacharjee T, Nakata T, Sasaki T, Kamado S and Hono K 2014 *Scr. Mater.* **90** 37
- [11] Edalati K, Yamamoto A, Horita Z and Ishihara T 2011 *Scr. Mater.* **64** 880.
- [12] Tsuji N, Ito Y, Saito Y and Minamino Y 2002 *Scr. Mater.* **47** 893
- [13] Barnett M 2007 *Mater. Sci. Eng. A* **464** 1
- [14] Koike J, Kobayashi T, Mukai T, Watanabe H, Suzuki M, Maruyama K and Higashi K 2003 *Acta Mater.* **51** 2055